Low Stability of Nucleocapsid Protein in SARS Virus†

Yulong Wang,‡ Xiaoyu Wu,‡ Yihua Wang, Bing Li, Hao Zhou, Guiyong Yuan, Yan Fu, and Yongzhang Luo*

Department of Biological Sciences and Biotechnology, MOE Laboratory of Protein Science, Tsinghua University, Beijing 100084, People's Republic of China

Received April 22, 2004; Revised Manuscript Received June 7, 2004

ABSTRACT: The nucleocapsid protein (N protein) is one of the major virion structural proteins of a newly identified coronavirus, which has been confirmed as the causative agent of severe acute respiratory syndrome (SARS). The major function of N protein is to assemble the RNA of coronavirus. In the present study, the gene encoding the N protein was cloned and the protein was expressed, purified, and refolded as shown by ^{1}H NMR measurement. The maximal Trp emission wavelength occurs near 331 nm, suggesting substantial burial of Trp residues. Circular dichroism measurements indicate that N protein contains little α-helical structure. Acid titration shows that N protein begins to unfold near pH 5 and is fully denatured near pH 2.7, and the acid unfolding process is reversible. The physical and chemical properties of N protein indicate that its stability is low. N protein is denatured reversibly at pH 7.4 either by urea (with C_m of 2.77 M and m value of 2.74 kcal mol^{-1} M^{-1}) or GdmCl (with C_m of 1.46 M and m value of 4.50 kcal mol^{-1} M^{-1}). In the heat-induced denaturation in phosphate-buffered saline buffer, N-protein starts to unfold at 35 °C and is completely denatured at 55 °C, where SARS virus was also reported to be inactivated. We propose that the low stability of N protein may be critical for the stability and function of SARS virus.

The coronaviruses (CoV)[1] are members of a family of enveloped viruses that replicate in the cytoplasm of animal host cells (*1*). They have a single-stranded plus-sense RNA genome approximately 30 kb in length with a 5′-cap structure and 3′-polyA tract (*1*). The entire genomic sequence of severe acute respiratory syndrome (SARS)−CoV has been reported (*2*-*4*). SARS−CoV contains open reading frames (ORF) for four structural proteins: nucleocapsid (N), spike (S), envelope (E), and membrane (M) protein (*2*−*5*). These four proteins are common to all known coronaviruses and play important roles during host cell entry, virion morphogenesis, and release (*6*). During virion assembly, N protein binds to a specific packaging signal on the viral RNA, leading to the formation of the helical nucleocapsid. Then the helical nucleocapsid interacts with M and E proteins to form the nucleocapsid complex, resulting in budding through the membrane (*6*).

The predicted N protein of SARS−CoV, with molecular weight of 46 kD and pI of 10.1, is a highly charged basic protein with high hydrophilicity (54%) and low hydrophobicity (17%) (*4*). Among all predicted structural proteins of SARS−CoV, N protein has the highest hydrophilicity and the highest pI, and it is the only one which does not have any cysteine residues; thus, it contains no disulfide bond. These features suggest that N protein may be less stable than other structural proteins of SARS−CoV. On the basis of the available information from other coronaviruses, nucleocapsid proteins are implicated in a variety of functions: in the replication of the genomic RNA (*7*, *8*), in the transcription of coronavirus subgenomic mRNAs (*9*, *10*), and in the translation from the subgenomic mRNAs (*11*). The stability of viral-specific proteins correlate directly with virus stability; for example, there are two mechanisms responsible for the inactivation of poliovirus, rhinovirus, and oral polio vaccine infectivity. One is the degradation of the viral capsid (protein denaturation), and the other is the degradation of the vRNA in the capsid (RNA inactivation) (*12*, *13*). Because N protein may have low stability, while it has multiple functions in SARS−CoV, moreover, no 3D structure of coronavirus nucleocapsid proteins has been elucidated yet. Studies on the stability of N protein may be useful in understanding the epidemiology of SARS.

MATERIALS AND METHODS

Materials. Ultrapure-grade GdmCl and urea were from Bebco. Ultrapure-grade glycine and MES were from Amresco. Molecular-biology-grade Tris base was from Promega. Analytically pure acetic acid, sodium acetate, sodium chloride, potassium chloride, disodium phosphate, potassium dihydrogen phosphate, and hydrochloride acid (HCl) were purchased from Beijing Yili.

Expression System. cDNA (BJ01) of SARS, a gift from Beijing Genomics Institute, was used as the template to amplify the N protein by polymerase chain reaction (PCR). The primers were 5′-CGG AAT TCC ATA TGT CTG ATA

† Supported in part by grants from Science and Technology Research Project of the Ministry of Education in China (03007), SARS program of Beijing Science and Technology Committee (H030230011020), and SARS Foundation (fd0303) of Tsinghua University.

* To whom correspondence should be addressed. Telephone: 86-10-6277-2897. Fax: 86-10-6279-4691. E-mail: protein@tsinghua.edu.cn.

‡ Y.W. and X.W. contributed equally to this study.

[1] Abbreviations: SARS, severe acute respiratory syndrome; CoV, coronavirus; N protein, nucleocapsid protein; FL, fluorescence; CD, circular dichroism; NMR, nuclear magnetic resonance; ISVP, infectious subvirion particles.

10.1021/bi049194b CCC: $27.50
Published on Web 08/06/2004

ATG GAC CCC AAT C-3′ and 5′-GGC CGA ATT CTT ATT ATG CCT GAG TTG AAT CAG CAG AA-3′. The PCR product was subcloned as an *Nde* I−*Eco*R I fragment into pET25b, and the fidelity of the construct pET25b-N was confirmed by DNA sequencing.

Protein Expression and Purification. Escherichia coli BL21(DE3) cells transformed with pET25b-N were grown at 37 °C in LB medium to an OD_{600} of 0.4−0.6 and induced with 0.4 mM isopropyl thio-β-D-galactopyranoside (IPTG) for 3.5 h. Cells were harvested by centrifugation and the cell pellets were resuspended and lysed by sonication in buffer A (50 mM Tris-HCl and 2 mM EDTA at pH 7.4) on ice. The cell lysate was centrifuged at 27000*g* for 20 min at 4 °C, and the supernatant was dialyzed into buffer B (10 mM NaH_2PO_4 and 1 mM EDTA at pH 7.4), and was then applied to an SP-Sepharose high-performance column (Pharmacia), which was pre-equilibrated with buffer B. The column was washed with 3 bed volumes of buffer B and then eluted by a linear gradient of NaCl from 0 to 0.8 M in buffer B. The purified protein was dialyzed into buffer B at 4 °C. The protein concentration was determined according to the method of Edelhoch (*14*).

pH Titration. A stock solution of N protein at pH 7 was aliquot into 4 mM acetate buffer at different pH values, using 1 M HCl to adjust the pH when pH values were lower than 3.5. The final protein concentration was 0.3 μM. After incubation of the samples at 25 °C for 20 min, fluorescence (FL) measurements were carried out. For the reversible refolding curve, N protein was first acid-denatured for 30 min at pH 1.5 and then pH titration was carried out according to the method mentioned above.

Reversible Denaturant-Induced Unfolding. A stock solution of N protein was added to aliquots with either GdmCl or urea of different concentrations, with a final protein concentration of 0.3 μM. The buffer was 5 mM Tris at pH 7.4. After incubation under 25 °C for 20 min, Trp FL measurements were carried out. For the reversible curves, N protein was first unfolded in 8 M urea or 6 M GdmCl for 30 min, respectively, and then the refolding curves were obtained as mentioned above.

Heat-Induced Unfolding. When performing heat-induced unfolding experiments, the temperature was gradually raised from 5 to 80 °C. At each temperature point, incubation for 10 min enables N protein to reach its equilibrium state and then FL measurement was carried out. The final protein concentration was 0.5 μM. The buffers for measuring thermal stability are 3 mM glycine-HCl for pH 2.0; 2 mM sodium acetate for pH 4.0; 3 mM MES for pH 6.0; 2 mM Tris or PBS (138 mM NaCl, 8 mM Na_2HPO_4, 1.5 mM KH_2PO_4, and 2.7 mM KCl) for pH 7.4; 2 mM Tris-HCl for pH 8.0; and 3 mM glycine-NaOH for pH 10.

FL Measurements. FL measurements were carried out using an F-4500 fluorescence spectrophotometer (Hitachi) in a cuvette with 1-cm light path. The excitation wavelength was 288 nm, and the emission data were collected between 300 and 400 nm. The slit widths for excitation and emission were 5 and 10 nm, respectively. All data were collected at 25 °C.

Circular Dichroism (CD) Measurements. CD measurements were performed on a Jasco-715 spectropolarimeter employing a 1-cm light-path cuvette, with the protein concentration of 1 μM. All data were collected at 25 °C.

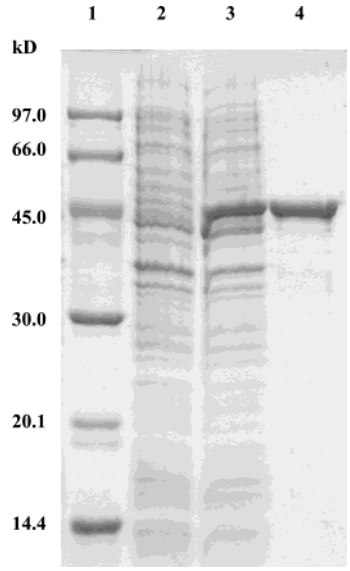

FIGURE 1: Expression and purification of N protein. The N protein was expressed in pET25b/BL21(DE3) and purified by SP-Sepharose HP. The expression and purification was monitored by 12% SDS−PAGE. Protein bands were stained with Coomassie brilliant blue. Lane 1, marker; lane 2, noninduced cell extract; lane 3, cell extract induced by 0.5 mM IPTG; and lane 4, purified N protein.

^{1}H NMR Measurements. N protein was dissolved in a solution containing 10% D_2O and 5 mM Tris-HCl at pH 7.4, with the protein concentration of 230 μM. ^{1}H NMR spectroscopy was performed at 500 MHz on a Varian Inova 500NB instrument at 25 °C. Spectra were acquired using a spectral width of 8000.0 Hz, a relaxation delay of 1.0 s, and 64 repetitions.

Data Analyses. The denaturant-induced unfolding curves were analyzed by assuming a two-state model with linear baselines, according to the procedure of Santoro and Bolen (*16*), which uses data inside as well as outside the transition zone to fix the baselines. The T_m values (the temperature midpoints of the thermal unfolding curves) were obtained using Microcal Origin software. The values of these parameters are the average of at least three unfolding experiments.

RESULTS

Expression and Purification of N Protein. The gene encoding N protein of SARS virus was cloned by PCR using the cDNA (BJ01) of SARS virus as the template. The N protein was then expressed in *E. coli* and purified by SP-Sepharose column to a purity of greater than 95% based on SDS−PAGE analysis (Figure 1). To test whether N protein is refolded, a ^{1}H NMR measurement was carried out at 25 °C and pH 7.4. We observed the upfield shifting of methyl peaks, dispersion in the aromatic region, and spreading out of the histidine $^1H^{\epsilon 1}$ resonances in the NMR spectrum of N protein (Figure 2a). All of these characters indicate a refolded tertiary structure, in agreement with studies of the denaturation of N protein (see below).

Spectroscopic Features of N Protein. N protein contains 5 tryptophan residues, and therefore we used Trp emission FL to monitor its unfolding process. Figure 2b shows the Trp FL emission spectra of N protein. The maximal emission wavelength occurs near 331 nm, which suggests substantial burial of Trp residues, and acid- or denaturant-induced unfolding cause a significant decrease in FL intensity and

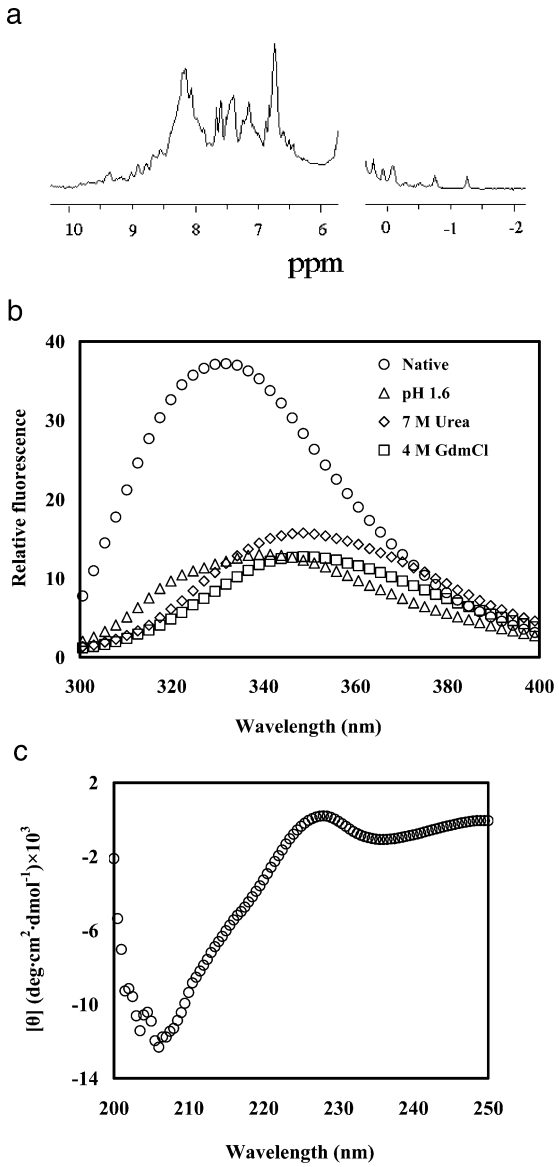

FIGURE 2: Spectroscopic features of N protein. (a) ^{1}H NMR spectrum at pH 7.4. (b) Trp emission FL spectrum of N protein at the native, acid-unfolded, urea-unfolded, and GdmCl-unfolded states, respectively. (c) CD spectrum at pH 7.4. All data were collected at 25 °C.

red shift of the maximal emission wavelength of N protein (Figure 2b). The CD spectrum indicate that N protein contains little α-helical structure (Figure 2c).

Acid Titration of N Protein. The pH titration curve of N protein at 25 °C shows that N protein begins to unfold near pH 5 and is fully denatured near pH 2.7 (Figure 3). Equilibrium for denaturation is reached within 10 min between pH 1 and 8, as is also true for denaturation induced by heat, urea, or GdmCl (see below). The acid-induced unfolding of N protein is S-shaped (Figure 3). When N protein is first denatured by acid at pH 1.5, it can refold back when pH is increased. The refolding curve overlaps well with the unfolding one (Figure 3), suggesting that the acid-unfolding process of N protein is reversible. For comparison, endostatin, an acid-resistant protein, starts to unfold around pH 3 and is completely denatured at pH 1.6 (*15*), and the denaturation process requires about 90 min to reach equilibrium for endostatin at pH 2. Thus, N protein is an acid-sensitive protein.

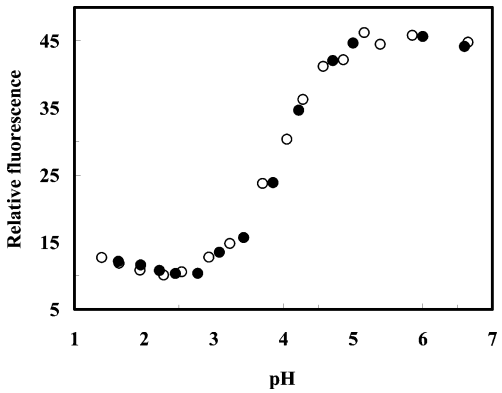

FIGURE 3: Acid-induced unfolding of N protein is reversible. The open and closed circles represent unfolding and refolding curves, respectively. Relative FL represents the Trp FL emission intensity at 330 nm after excitation at 288 nm. Protein concentration was 0.3 μM. The buffer was 4 mM NaAc/HAc. All measurements were carried out at 25 °C.

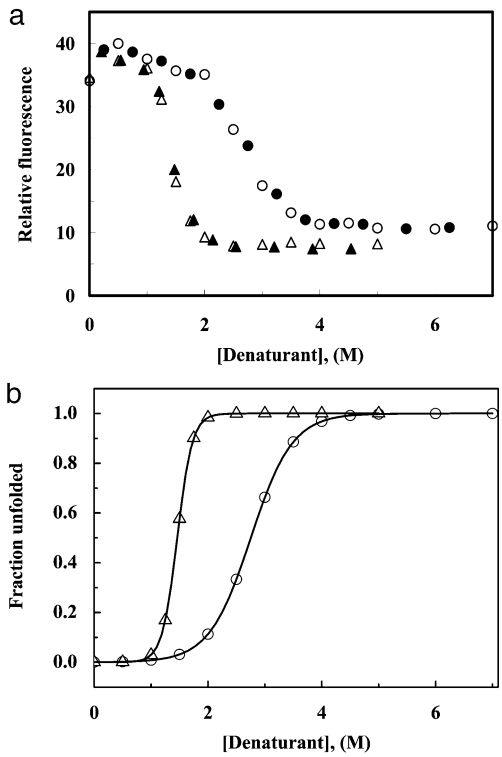

FIGURE 4: Denaturant-induced unfolding of N protein is reversible. The denaturants are urea (○ and ●) and GdmCl (△ and ▲), respectively. Relative FL represents the Trp FL emission intensity at 330 nm after excitation at 288 nm. Open and closed symbols represent unfolding and refolding curves, respectively. All data were collected at pH 7.4 and 25 °C, with the final protein concentration of 0.3 μM. (a) Raw data, and (b) normalized data of unfolding curves.

Denaturant-Induced Unfolding of N Protein. Two denaturants, urea and GdmCl, were used to measure the stability of N protein at pH 7.4 and 25 °C. The unfolding curves are also reversible (Figure 4a) and can be fitted to the two-state model of Santoro and Bolen (*16*) (Figure 4b). The C_m value (the denaturant molarity at the midpoint of the transition) is 2.77 and 1.46 M for urea and GdmCl, respectively. The *m* values (the cooperativity index of the transition; see Materials and Methods) are 2.74 kcal mol^{-1} M^{-1} for urea and 4.50 kcal mol^{-1} M^{-1} for GdmCl. These parameters suggest that GdmCl is more powerful in denatur-

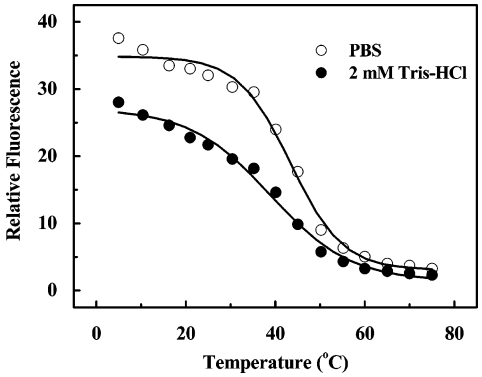

FIGURE 5: Thermostability measurements of N protein monitored by Trp emission FL at 330 nm. Heat-induced unfolding was carried out in PBS or 2 mM Tris buffer, with the final protein concentration of 0.5 μM.

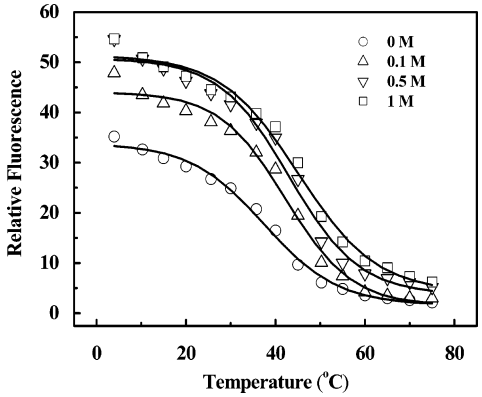

FIGURE 6: Thermostability measurements of N protein at different concentrations of NaCl at pH 8.0 monitored by Trp emission FL at 330 nm. The concentrations of NaCl are 0, 0.1, 0.5, and 1.0 M.

ing N protein and that the unfolding process by GdmCl is more cooperative. For comparison, the urea C_m values are 8.54 M for lysozyme (pH 4 and 30 °C) (*17*), 6.98 M for RNase A (pH 8 and 30 °C) (17), and 4.79 M for β-lactoglobulin (pH 3.2 and 25 °C) (*18*). This comparison indicates that the SARS N protein is marginally stable. CD is often used to monitor the denaturation reactions of proteins (*17*, *19*, *20*), but CD is not a sensitive probe of the denaturant-induced unfolding of N protein, probably because of its low α-helical content. Thus, we did not carry out CD-monitored unfolding of N protein.

Heat-Induced Unfolding of N Protein. In PBS buffer, N protein starts to unfold around 35 °C and is completely unfolded around 55 °C, with a T_m of 43 °C (Figure 5). Heat-induced denaturation of N protein is reversible; when N protein is denatured completely at 55 °C in PBS buffer for more than 30 min, it can refold back to its native state at 25 °C (data not shown). The heat-induced unfolding curves of N protein are S-shaped.

Because PBS contains large amount of salts, we decided to carry out the heat-induced denaturation of N protein in 2 mM Tris-HCl at low ionic strength. Considering that Tris buffer shows significant pH dependence on temperature (*21* and the references therein), the pH in Tris buffer was actually measured at each temperature as indicated. N protein is more sensitive to temperature in 2 mM Tris-HCl, compared to PBS (Figure 5). It begins to unfold near 30 °C and is completely unfolded at 50 °C. The T_m is 38 °C, which is a very low value.

Effect of Anions on the Stability of N Protein. Because the T_m values increase from 38 °C in 2 mM Tris buffer to 43 °C in PBS buffer (Figure 5), apparently the rise in T_m is caused by chloride. To study the effect of anions on the stability of N protein, two kinds of anions are chosen, chloride and sulfate. Thermal-induced unfolding of N protein at different concentrations of NaCl at pH 8.0 shows that the stability of N protein increases with NaCl concentrations from 0 to 1 M (Figure 6). The effect of different concentrations of NaCl on the thermal stability of N protein at pH values of ~4−10 is shown in Figure 7. The stability of N protein increases with NaCl concentrations from 0 to 1 M from pH 4−8, with more significant effect at pH 8 than at lower pH values (Figure 7). Interestingly, N protein becomes less stable at pH 10 than at pH 8 at NaCl concentrations

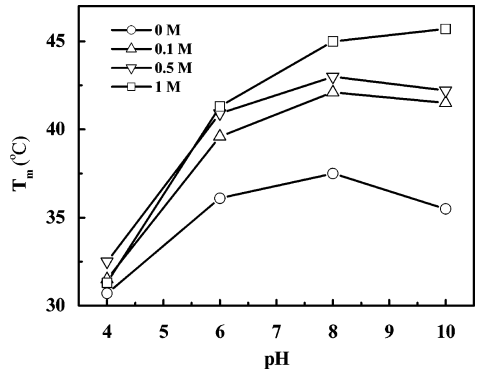

FIGURE 7: Effect of different concentrations of NaCl on the thermostability of N protein from pH 4 to 10 monitored by Trp emission FL at 330 nm. The T_m was determined from the primary data using Origin (Microcal software). For buffers, see Materials and Methods.

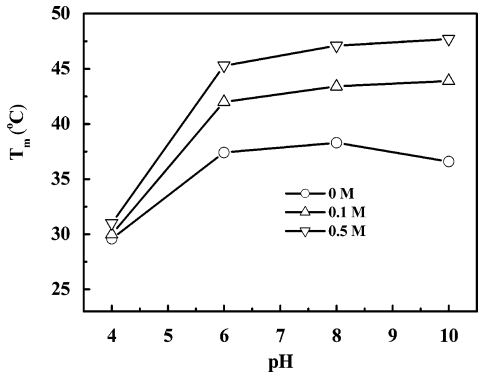

FIGURE 8: Effect of different concentrations of Na_2SO_4 on the thermostability of N protein from pH 4 to 10 monitored by Trp emission FL at 330 nm. The T_m was determined from the primary data using Origin (Microcal software). For buffers, see Materials and Methods.

from 0 to 0.5 M, with an exception of NaCl at 1.0 M, at which N protein is slightly more stable at pH 10 than at pH 8. The largest increase in the stability of N protein is observed at pH 10 at NaCl concentrations from 0 to 1 M (Figure 7).

Similar stabilizing effects are observed when Na_2SO_4 is present at concentrations from ~0−0.5 M (Figure 8), and the largest increase in the stability of N protein is also observed at pH 10.

DISCUSSION

Anion Stabilization of N Protein. Anions can stabilize proteins either by binding to proteins, through which the net positive charges on the protein can be reduced, which is considered to be a characteristic property of molten globules or native proteins (*22*−*24*), or by shielding destabilizing electrostatic interactions (*25*, *26*). Two anions, which differ widely in their effectiveness in stabilizing molten globules or proteins, are studied here: sulfate, which stabilizes molten globules at low salt concentrations, and chloride, which stabilizes them at considerably higher salt concentrations (*27*). At a given molar concentration, the ionic strength of a Na_2SO_4 solution is three times larger than that of a NaCl solution. Both anions can stabilize native ribonuclease A at low pH (*25*) and molten globule forms of cytochrome *c* and apomyoglobin (*27*).

Here, we find that N protein can be stabilized by these two anions at pH from 4 to 10. Because the predicted N protein has a high pI value of 10.1 (*4*), the net charge of N protein at pH 10 should be near 0; thus, the anion-binding effect is not likely. With the decreasing pH, the net charge of N protein increases. Our results (Figures 7 and 8) surprisingly show that both the two anions have a more stabilizing effect on N protein at higher pH, in contrast to most of the other observations that the anion-stabilizing effect is normally greater at lower pH if anion binding plays a major role (*25*). We thus conclude that the anion-binding effect is not likely to play a major role in N protein. The increase in T_m is 10 °C between 0 and 1 M NaCl and 11 °C between 0 and 0.5 M Na_2SO_4, respectively, and may be caused mainly by shielding destabilizing electrostatic interactions. At pH 4, where N protein is nearly denatured by acid (Figure 3), the T_m is almost independent of the concentration of salts (Figures 7 and 8). We have also observed that salts have no effect on the T_m of N protein at pH 2 (data not shown). These findings suggest that salts have a stabilizing effect on native N protein but not on denatured N protein.

Stability Correlation between N Protein and SARS Virus. Dimmock showed that poliovirus and rhinovirus could be inactivated through damage to both the viral capsid (protein denaturation) or to the viral RNA inside the capsid (RNA inactivation) (*12*). There are two mechanisms that are responsible for the extensive drop in viral infectivity upon moderate heating (42−45 °C) of oral polio vaccine. One of the mechanisms is the degradation of the viral capsid (protein denaturation). The other is the degradation of the vRNA in the capsid (RNA inactivation) (*13*). Jané-Valbuena et al. (*28*) showed that T1L infectious subvirion particles (ISVPs) of reovirus are less thermostable than T1L virions at 52 °C but the "recoated" T1L ISVPs with the σ3 (outer-capsid protein) in vitro are as thermostable as virions at that temperature. This finding indicates that σ3 is an important determinant of the thermostability of virions. Another insight into the thermal inactivation of reovirus particles was obtained from the finding that mutants of reovirus T3D selected for resistance to ethanol and attributed to mutations in the μ1 outer-capsid protein (*29*) showed an increase in the thermostability of their ISVPs, suggesting that μ1 is an important determinant of the thermostability of particles that lack σ3 (*30*).

It is well-known that proteins isolated from thermophilic bacteria can display lower melting temperatures in vitro than the temperature at which the bacteria thrive (*31*). Presumably, the in vivo context alters the thermodynamic properties of these proteins such that their inherent stabilities are increased. Similarly, the nucleocapsid context for N protein could render it more stable than observed in isolation. Because the interactions between N protein and viral RNAs are important in RNA transcription, genome replication, encapsidation, and translation, it would be important to measure the thermostability of N protein in vivo when SARS virus is subjected to thermal stress. However, this is impractical at present because of the danger of infection for performing such studies. Nevertheless, the thermostability of N protein was not affected when single-stranded DNA for the S protein of SARS virus was present (data not shown).

Duan and his colleagues reported that SARS virus lost its infectious capacity at 56 °C (*32*). Our studies show that the low stability of N protein may be at least one of the important determinants for the thermostability of SARS virus. In the thermal-induced unfolding in PBS buffer, SARS N protein begins to unfold at 35 °C and is completely denatured at 55 °C, with a T_m value of 43 °C. This completely thermodenatured temperature of 55 °C of N protein coincides well with the fact that SARS virus is completely noninfectious around 55 °C (*32*).

ACKNOWLEDGMENT

We gratefully acknowledge R. L. Baldwin and members of the Luo laboratory for insightful discussions and criticism throughout the course of this work and Beijing Genomics Institute for the cDNA (BJ01) of SARS.

REFERENCES

1. Fields, B. N., Knipe, D. M., Howley, P. M., and Griffin, D. E. (2001) *Fields Virology*, 4th ed., Lippincott Williams and Wilkins, Philadelphia, PA.
2. Marra, M. A., Jones, S. J., Astell, C. R., Holt, R. A., Brooks-Wilson, A., Butterfield, Y. S., Khattra, J., Asano, J. K., Barber, S. A., Chan, S. Y., Cloutier, A., Coughlin, S. M., Freeman, D., Girn, N., Griffith, O. L., Leach, S. R., Mayo, M., McDonald, H., Montgomery, S. B., Pandoh, P. K., Petrescu, A. S., Robertson, A. G., Schein, J. E., Siddiqui, A., Smailus, D. E., Stott, J. M., Yang, G. S., Plummer, F., Andonov, A., Artsob, H., Bastien, N., Bernard, K., Booth, T. F., Bowness, D., Czub, M., Drebot, M., Fernando, L., Flick, R., Garbutt, M., Gray, M., Grolla, A., Jones, S., Feldmann, H., Meyers, A., Kabani, A., Li, Y., Normand, S., Stroher, U., Tipples, G. A., Tyler, S., Vogrig, R., Ward, D., Watson, B., Brunham, R. C., Krajden, M., Petric, M., Skowronski, D. M., Upton, C., and Roper, R. L. (2003) The genome sequence of the SARS-associated coronavirus, *Science 300*, 1399−1404.
3. Rota, P. A., Oberste, M. S., Monroe, S. S., Nix, W. A., Campagnoli, R., Icenogle, J. P., Penaranda, S., Bankamp, B., Maher, K., Chen, M. H., Tong, S., Tamin, A., Lowe, L., Frace, M., DeRisi, J. L., Chen, Q., Wang, D., Erdman, D. D., Peret, T. C., Burns, C., Ksiazek, T. G., Rollin, P. E., Sanchez, A., Liffick, S., Holloway, B., Limor, J., McCaustland, K., Olsen-Rasmussen, M., Fouchier, R., Gunther, S., Osterhaus, A. D., Drosten, C., Pallansch, M. A., Anderson, L. J., and Bellini, W. J. (2003) Characterization of a novel coronavirus associated with severe acute respiratory syndrome, *Science 300*, 1394−1399.
4. Qin, E. D., Zhu, Q. Y., Yu, M., Fan, B. C., Chang, G. H., Si, B. Y., Yang, B. A., Peng, W. M., Jiang, T., Liu, B. H., Deng, Y. Q., Liu, H., Zhang, Y., Wang, C. E., Li, Y. Q., Gan, Y. H., Li, X. Y., Lü, F. H., Tan, G., Cao, W. C., and Yang, R. F. (2003) A complete sequence and comparative analysis of a SARS-associated virus (isolate BJ01), *Chin. Sci. Bull. 48*, 10941−10948.

5. Holmes, K. V., and Enjuanes, L. (2003) The SARS coronavirus: A postgenomic era, *Science 300*, 1377−1378.
6. Siddell, S. G., Ed. (1995) *The Coronaviridae*, Plenum, New York.
7. Chang, R. Y., and Brian, D. A. (1996) *cis* Requirement for N-specific protein sequence in bovine coronavirus defective interfering RNA replication, *J. Virol. 70*, 2201−2207.
8. Compton, S. R., Rogers, D. B., Holmes, K. V., Fertsch, D., Remenick, J., and McGowan, J. J. (1987) *In vitro* replication of mouse hepatitis virus strain A59, *J. Virol. 61*, 1814−1820.
9. Baric, R. S., Nelson, G, W., Fleming, J. O., Deans, R. J., Keck, J. G., Casteel, N., and Stohlman, S. A. (1988) Interaction between coronavirus nucleocapsid protein and viral RNAs: Implications for viral transcription, *J. Virol. 62*, 4280−4287.
10. Stohlman, S. A., Baric, R. S., Nelson, G. N., Soe, L. H., Welter, L. M., and Deans, R. J. (1988) Specific interaction between coronavirus leader RNA and nucleocapsid protein, *J. Virol. 62*, 4288−4295.
11. Ulmanen, I., Sodderlund, H., and Kaarianen, L. (1976) Forest virus capsid protein associates with 60S ribosomal subunit in infected cells, *J. Virol. 20*, 203−210.
12. Dimmock, N. J. (1967) Differences between the thermal inactivation of picornaviruses at "high" and "low" temperatures, *Virology 31*, 338−353.
13. Rombaut, B., Verheyden, B., Andries, K., and Boeyé A. (1994) Thermal inactivation of oral polio vaccine: Contribution of RNA and protein inactivation, *J. Virol. 68*, 6454−6457.
14. Edelhoch, H. (1967) Spectroscopic determination of tryptophan and tyrosine in proteins, *Biochemistry 6*, 1948−1954.
15. Li, B., Wu, X., Zhou, H., Chen, Q., and Luo, Y. (2004) Acid-induced unfolding mechanism of recombinant human endostatin, *Biochemistry 43*, 2550−2557.
16. Santoro, M. M., and Bolen, D. W. (1988) Unfolding free energy changes determined by the linear extrapolation method. 1. Unfolding of phenylmethanesulfonyl α-chymotrypsin using different denaturants, *Biochemistry 27*, 8063−8068.
17. Luo, Y., and Baldwin, R. L. (1998) Trifluoroethanol stabilizes the pH 4 folding intermediate of sperm whale apomyoglobin, *J. Mol. Biol. 279*, 49−57.
18. Arai, M., Ikura, T., Semisotnov, G. V., Kihara, H., Amemiya, Y., and Kuwajima, K. (1998) Kinetic refolding of β-lactoglobulin. Studies by synchrotron X-ray scattering, and circular dichroism, absorption, and fluorescence spectroscopy, *J. Mol. Biol. 275*, 149−162.
19. Luo, Y., Kay, M. S., and Baldwin, R. L. (1997) Cooperativity of folding of the apomyoglobin pH 4 intermediate studied by glycine and proline mutations, *Nat. Struct. Biol. 4*, 925−930.
20. Luo, Y., and Baldwin, R. L. (1999) The 28−111 disulfide bond constrains the α-lactalbumin molten globule and weakens its cooperativity of folding, *Proc. Natl. Acad. Sci. U.S.A. 96*, 11283−11287.
21. Fukada, H., and Takahashi, K. (1998) Enthalpy and heat capacity changes for the proton dissociation of various buffer components in 0.1 M potassium chloride, *Proteins 33*, 159−166.
22. Makhatadze, G. I., Lopez, M. M., Richardson, J. M., III, and Thomas, S. T. (1998) Anion binding to the ubiquitin molecule, *Protein Sci. 7*, 689−697.
23. Bedell, J. L., McCrary, B. S., Edmondson, S. P., and Shriver, J. W. (2000) The acid-induced folded state of Sac7d is the native state, *Protein Sci. 9*, 1878−1888.
24. Sakurai, K., Oobatake, M., and Goto, Y. (2001) Salt-dependent monomer−dimer equilibrium of bovine β-lactoglobulin at pH 3, *Protein Sci. 10*, 2325−2335.
25. Ramos, C. H. I., and Baldwin, R. L. (2002) Sulfate anion stabilization of native ribonuclease A both by anion binding and by the Hofmeister effect, *Protein Sci*. *11*, 1771−1778.
26. Jencks, W. P. (1987) Catalysis, in *Chemistry and Enzymology*, pp 358−392, Dover, Mineola, NY.
27. Goto, Y., Calciano, L. J., and Fink, A. L. (1990) Acid-induced folding of proteins, *Proc. Natl. Acad. Sci. U.S.A. 87*, 573−577.
28. Jané-Valbuena, J., Nibert, M. L., Spencer, S. M., Walker, S. B., Baker, T. S., Chen, Y., Centonze, V. E., and Schiff, L. A. (1999) Reovirus virion-like particles obtained by recoating infectious subvirion particles with baculovirus-expressed σ3 protein: An approach for analyzing σ3 functions during virus entry, *J. Virol. 73*, 2963−2973.
29. Wessner, D. R., and Fields, B. N. (1993) Isolation and genetic characterization of ethanol-resistant reovirus mutants, *J. Virol. 67*, 2442−2447.
30. Hooper, J. W., and Fields, B. N. (1996) Role of the μ1 protein in reovirus stability and capacity to cause chromium release from host cells, *J. Virol. 70*, 459−467.
31. Kumar, S., and Nussinov, R. (2001) How do thermophilic proteins deal with heat? *Cell. Mol. Life Sci. 58*, 1216−1233.
32. Duan, S. M., Zhao, X. S., Wen, R. F., Huang, J. J., Pi, G. H., Zhang, S. X., Han, J., Bi, S. L., Ruan, L., Dong, X. P., and SARS Research Team (2003) Stability of SARS coronavirus in human specimen and environment and its sensitivity to heating and UV irradiation, *Biomed. Environ. Sci. 16*, 105−111.

BI049194B